verified by independently observing the spectrum of (OEP)-Fe^{III}(1,4-$OC_6Cl_2(CN)_2O$)Fe^{III}(OEP).) These features are emphasized in the insets in Figure 4. These observations assure us that the species being observed in these NMR spectra are the intact, dimeric species. Additionally, we have noted that there is no concentration dependence of these spectra, whereas dissociation should produce concentration effects.

Asymmetry can also be introduced into these species by employing an unsymmetrical quinone. Figure 5 shows the spectrum obtained by using reaction 1 with 2,6-dimethyl-1,4-benzoquinone (R, R'' = H; R', R''' = CH_3). The spectrum clearly shows two equally intense pyrrole resonances at 62 and 64 ppm along with a broad resonance at 70 ppm due to the methyl groups of the bridging ligand. The other two protons of that bridge were not seen; presumably they were too broad. Similarly, splitting of the pyrrole resonances was also observed with the diiron complex formed from 2,3-dimethoxy-5-methyl-1,4-benzoquinone (coenzyme Q_0; R, R' = OMe, R'' = Me, R''' = H).

Experimental Section

Materials. Substituted quinones were obtained from Aldrich Chemicals, and the diiron complexes were obtained via reaction 1 according to the method of Kessel and Hendrickson.[2] The sample used to obtain the spectrum shown in trace C of Figure 1 was prepared by heating a mixture of (TTP)$Fe^{III}OFe^{III}$(TTP) and excess *p*-hydroquinone in toluene-d_8 for 1 h at 80 °C in an NMR tube.

Instrumentation. NMR spectra were recorded on Nicolet NT-360 FT and GE QE-300 spectrometers operating in the quadrature mode (^1H frequencies are 360 and 300 MHz, respectively). The spectra were collected over a 40-kHz bandwidth with 16K data points and a 6-μs 90° pulse. For a typical paramagnetic spectrum, between 500 and 2000 transients were accumulated with a delay time of 50 ms. The signal-to-noise ratio was improved by apodization of the free induction decay. The residual methyl peak of toluene was used as a secondary reference, which was set at 2.09 ppm.

Acknowledgment. We thank the National Institutes of Health (Grant GM-26226) for support.

Registry No. (TTP)Fe^{III}(1,4-$O_2C_6H_4$)Fe^{III}(TTP), 128471-79-4; (TTP)Fe^{III}(1,4-$O_2C_6Cl_4$)Fe^{III}(TTP), 128471-80-7; (TTP)Fe^{III}(1,4-O_2C_6-(2,3-Cl)(5,6-CN))Fe^{III}(TTP), 128471-81-8; (TTP)Fe^{III}(1,4-$O_2C_6Me_4$)-Fe^{III}(TTP), 128471-82-9; (TTP)Fe^{III}(1,4-$O_2C_6H_2$(2,6-Me))Fe^{III}(TTP), 128471-83-0; (TTP)Fe^{III}(1,4-O_2C_6(2,3-MeO)(5-Me))Fe^{III}(TTP), 128471-84-1.

Contribution from the Department of Chemistry, National Taiwan University, Taipei, Taiwan, ROC

Charge Density Study of Thiourea *S,S*-Dioxide

Yu Wang,* Ning-Leh Chang, and Ching-Tzong Pai

Received October 3, 1989

Thiourea *S,S*-dioxide has been studied by X-ray diffraction at room temperature.[1,2] The unusually long carbon–sulfur bond was noticed,[1] and a suggestion of mesoionic character with a positive charge located on the $(NH_2)_2C$ part and a negative charge on the SO_2 part of the molecule was made.[1] Dunitz[3] gave an explanation that the weakening of the carbon–sulfur p_σ–p_σ bond[1,3] is due to the odd electron of SO_2^- being of d_π character. In order to understand the bonding character of this molecule, a deformation density study was undertaken. The same approach was applied to the thiourea molecule, where the electron density distribution was studied both experimentally and theoretically in detail.[4-8] It would be a nice comparison between thiourea and thiourea dioxide to see the difference in the C–S bond as well as in the long-pair region of the sulfur atom. The strong hydrogen bonds in this crystal are also of interest.

* To whom correspondence should be addressed.

Table I. Crystal Data for Thiourea *S,S*-Dioxide

chem formula	$(H_2N)_2CSO_2$	fw	110
a, Å	10.719 (2)	space group	*Pnma* (No. 62)
b, Å	10.109 (2)	μ, cm^{-1}	6.10
c, Å	3.8018 (7)	λ, Å	0.7107
D_{calcd}, $g\cdot cm^{-3}$	1.743	transm coeff	0.74–0.89
V, $Å^3$	411.9	$R(F)$	0.0225, 0.0183[a]
Z	4	$R_w(F)$	0.0363, 0.0233[a]
T, K	110		

[a] High-order refinement.

Table II. Atomic Fractional Coordinates and B(eq) ($Å^2$)

atom	refinement	*x*	*y*	*z*	B(eq)[d]
S	*a*	0.460 52 (1)	0.25	0.361 01 (4)	0.827 (5)
	b	0.460 54 (8)	0.25	0.361 06 (3)	0.811 (4)
	c	0.460 55 (1)	0.25	0.361 05 (2)	0.810 (3)
C	*a*	0.611 62 (4)	0.25	0.601 19 (15)	0.818 (12)
	b	0.611 67 (3)	0.25	0.601 29 (11)	0.799 (8)
	c	0.611 68 (3)	0.25	0.601 30 (10)	0.809 (9)
N	*a*	0.663 61 (3)	0.364 77 (3)	0.664 77 (11)	1.082 (10)
	b	0.663 57 (2)	0.364 70 (3)	0.664 71 (8)	1.070 (6)
	c	0.663 59 (2)	0.364 63 (3)	0.664 85 (9)	1.071 (7)
O	*a*	0.401 79 (3)	0.127 48 (3)	0.509 54 (10)	1.093 (9)
	b	0.401 73 (2)	0.127 67 (2)	0.509 68 (7)	1.074 (6)
	c	0.401 73 (2)	0.127 58 (3)	0.509 60 (9)	1.074 (7)
H1	*a*	0.737 0 (7)	0.369 6 (9)	0.768 (3)	1.78 (16)
	b	0.746 92	0.370 23	0.781 97	1.78
H2	*a*	0.628 8 (7)	0.432 2 (11)	0.626 5 (24)	1.72 (17)
	b	0.619 64	0.450 05	0.616 36	1.72

[a] From full data refinement. [b] From high-angle data ($(\sin\theta)/\lambda > 0.65$) refinement. [c] From multipole refinement. [d] $B(eq) = (8/3)\pi^2\sum_i\sum_j U(i,j)a_i^*a_j^*\cdot a_i a_j$.

Experimental Section

The title compound was prepared by oxidizing thiourea with 3% hydrogen peroxide at 0 °C for 3 h and crystallized in an aqueous solution.

The crystal data of $(NH_2)_2CSO_2$ at 110 K are listed in Table I. The intensity data were collected on a CAD4 diffractometer equipped with a graphite monochromator and liquid-N_2 gas flow set up using Mo Kα radiation. A sealed box was designed[9] with a dry ice/acetone cold trap to ensure a low humidity around the crystal. Some of the experimental details are given in Table I. The intensity data were measured up to $2\theta = 100°$ for two equivalent sets of reflections (hkl, $\bar{h}kl$). Five measurements at ψ values from −30 to 30° with a step of 15° were collected for each reflection up to $2\theta = 60°$. An additional equivalent set of reflections ($hk\bar{l}$) was collected up to $2\theta = 90°$. This yielded a total of 8676 measurements, which gave 2224 unique reflections after averaging of equivalents. The interest agreement is 2.1%. Three standard reflections monitored every 1 h showed variations of less than ±5%. An absorption correction was applied according to 10 measured faces of the compound. The crystal size is large in one direction, but cutting of the crystal would cause crystal damage. The collimator size was adjusted to ensure that the crystal was in the beam. All of the computations were carried out on a local MicroVAXIII computer using mainly NRCVAX programs.[10] The refinements of the multipole model were also carried out on the MicroVAX computer using the MOLLY program.[11] Both least-squares refinements are based on F_o, with weight calculated as $1/[\sigma^2(F_o) +$

(1) Sullivan, R. L.; Hargreaves, A. *Acta Crystallogr.* **1962**, *15*, 675.
(2) Chen, I. C.; Wang, Y. *Acta Crystallogr., Sect. C: Cryst. Struct. Commun.* **1984**, *C40*, 1890.
(3) Dunitz, J. D. *Acta Crystallogr.* **1956**, *9*, 579.
(4) Mullen, D.; Hellner, E. *Acta Crystallogr., Sect. B: Struct. Crystallogr. Cryst. Chem.* **1978**, *B34*, 2789.
(5) Mullen, D.; Scheringer, C. *Acta Crystallogr., Sect. A: Cryst. Phys., Diffr., Theor. Gen. Crystallogr.* **1978**, *A34*, 476.
(6) Kutoglu, A.; Scheringer, C.; Meyer, H.; Schweig, A. *Acta Crystallogr., Sect. B: Struct. Sci.* **1982**, *B38*, 2626.
(7) Breitenstein, M.; Dannohl, H.; Meyer, H.; Schweig, A.; Seeger, R.; Seeger, U.; Zittlau, W. *Intl. Rev. Phys. Chem.* **1983**, *3*, 335.
(8) Mullen, D. *Acta Crystallogr., Sect. B: Struct. Sci.* **1982**, *B38*, 2620.
(9) Ueng, C. H. Ph.D. Thesis, National Taiwan University, 1987.
(10) Gabe, E. J.; Lee, F. L.; LePage, Y. *Crystallographic Computing 3*; Sheldrick, G. M., Kruger, C., Goddard, R., Eds.; Clarendon Press: Oxford, England, 1985; pp 167–174.
(11) Hansen, N. H.; Coppens, P. *Acta Crystallogr., Sect. A: Cryst. Phys., Diffr., Theor. Gen. Crystallogr.* **1978**, *A34*, 909.

0020-1669/90/1329-3256$02.50/0

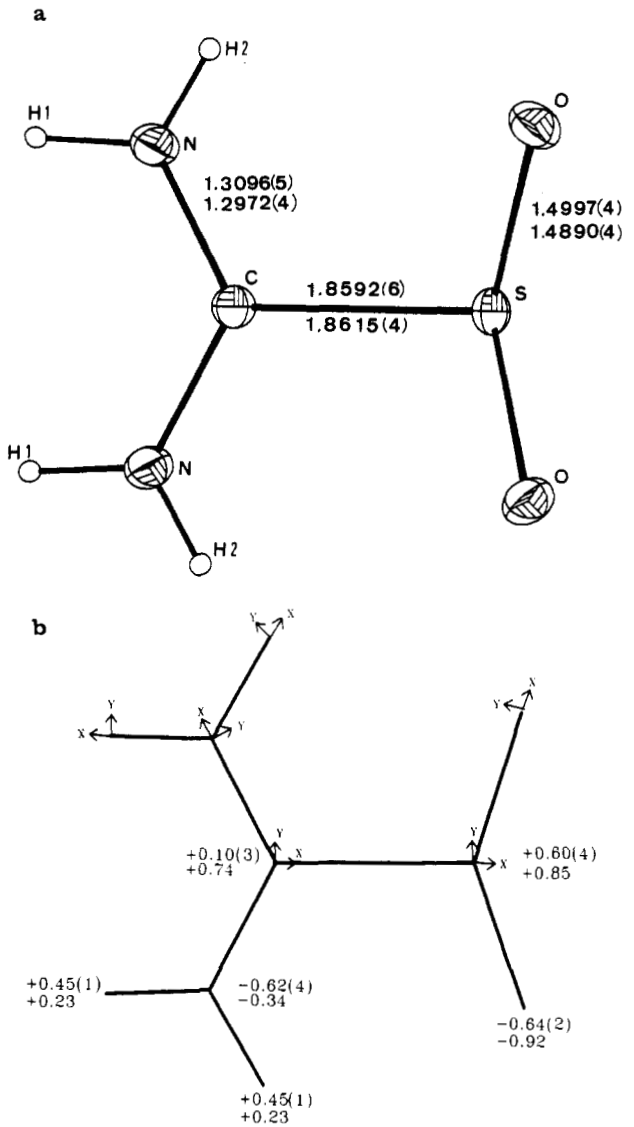

Figure 1. (a) Molecular drawing with thermal ellipsoids (50% probability) at 110 K. Bond lengths (Å) at 110 K (top) and 300 K (bottom). (b) Choice of local Cartesian axes for the multipole refinements. The numbers near the atoms are the net charges obtained from multipole refinement (top) and from EHMO (bottom).

$(0.01F_o)^2$]. An additional multipole refinement based on F^2 was also performed; the results were similar but gave slightly higher agreement indices. The deformation density maps generated both from the normal refinement and from the multipole refinement were produced by a locally developed contour-plotting program.[12]

Results

The atomic parameters from the full data refinement and the high-order refinement ($(\sin\theta)/\lambda > 0.65$ Å^{-1}) using the spherical atom model are given in Table II. The thermal ellipsoids of the molecule at 110 K and the bond lengths at both 110 and 300 K are shown in Figure 1a. The thermal parameters of the nonhydrogen atoms decrease to 30% on average by lowering the temperature from 300 to 110 K. However, the anisotropy in the thermal vibrations did not change significantly. The atomic scattering factors, f_o, were calculated from the analytical expression, with the coefficients taken from ref 13b. Anomalous dispersion corrections were applied according to ref 13a.

The experimental deformation density is calculated as the difference between the observed density, ρ_{obs}, and the superposition of the sum of spherically averaged free atom densities, $\sum\rho_c$. The deformation densities were calculated up to a resolution of (sin $\theta)/\lambda$ = 1.08 Å^{-1}. The Fourier coefficients were taken to be the differences between kF_o and F_c values calculated with the atomic parameters obtained from the high-order ($(\sin\theta)/\lambda > 0.65$ Å^{-1}) refinement. The hydrogen positions were displaced[14-16] along the N–H vector to make the N–H distance of 1.0 Å.[13a] Here k is the optimum scale factor for the data used in the Fourier synthesis ($(\sin\theta)/\lambda$ = 0–1.08 Å^{-1}).

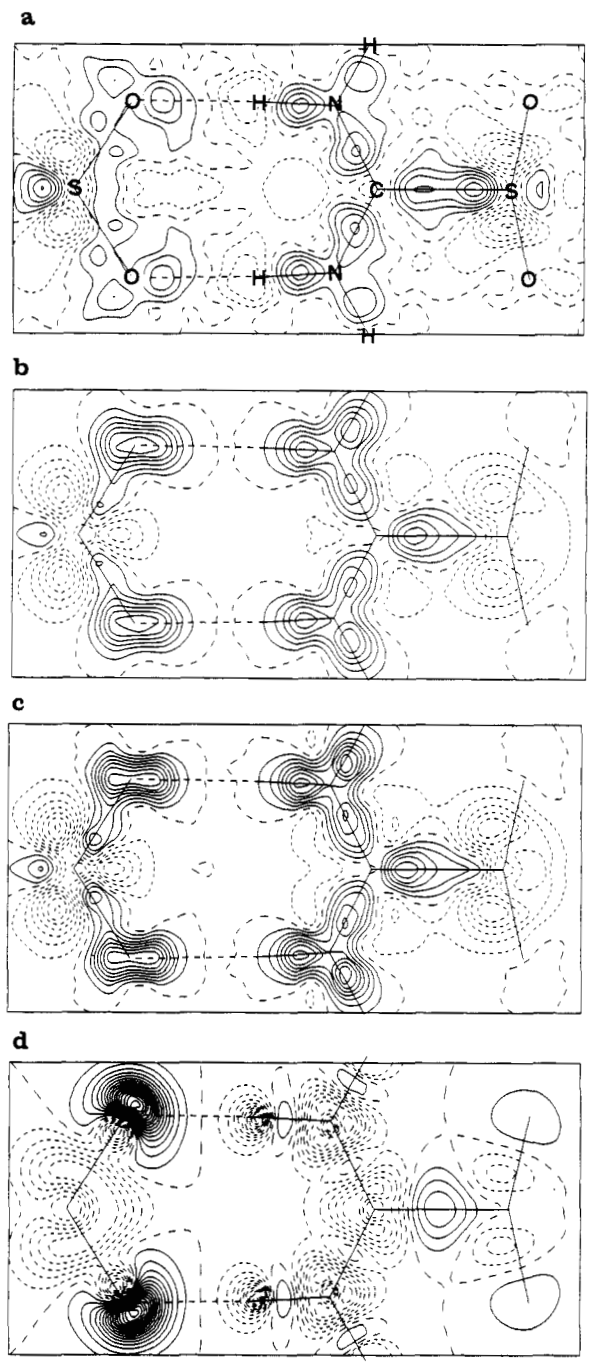

Figure 2. Deformation density maps of the thiourea plane and plane of NN'S (carbon atom 0.064 Å off the plane contour level): 0.1 e/Å^3; solid lines positive, dashed and dotted lines zero and negative. Key: (a) X – X(high); (b) X(multipole) – X(spherical), dynamic; (c) X(multipole) – X(spherical), static; (d) $\rho_{mo} - \sum\rho_{ao}$ from EHMO.

The experimental deformation electron density distribution for the plane of the thiourea part with a nearly coplanar SO_2 fragment

(12) Tsai, C. J. Masters Thesis, National Taiwan University, 1982.
(13) *International Tables for X-ray Crystallography*; Kynoch: Birmingham, England, 1974: (a) Vol. III; (b) Vol. IV.
(14) Wang, Y.; Angermund, K.; Goddard, R.; Kruger, C. *J. Am. Chem. Soc.* **1987**, *109*, 1587.
(15) Wang, Y.; Guo, L. W.; Lin, H. C.; Kao, C. T.; Tsai, C. J.; Bats, J. W. *Inorg. Chem.* **1988**, *27*, 520.
(16) Wang, Y.; Chen, M. J.; Wu, C. H. *Acta Crystallogr., Sect. B: Struct. Sci.* **1988**, *B44*, 179.

Table III. Least-Squares Results of Multipole Refinements (Based on F)

	NV[a]	R_1[b]	R_2[b]	R_{1w}[b]	R_{2w}[b]	S
conventional	32	0.0286	0.0498	0.0522	0.0687	3.47
monopole	41	0.0240	0.0424	0.0373	0.0581	2.49
octapole	92	0.0181	0.0332	0.0227	0.0498	1.54
octapole[c]	97	0.0174	0.0317	0.0217	0.0468	1.47
hexadecapole	120	0.0171	0.0313	0.0210	0.0447	1.43

[a] NV = number of variables. [b] $R_1 = \sum||F_o| - k|F_c||/\sum|F_o|$. $R_2 = \sum|F_o^2 - kF_o^2|/\sum F_o^2$. $R_{1w} = [\sum w(|F_o| - k|F_c|)^2/\sum wF_o^2]^{1/2}$. $R_{2w} = [\sum w|F_o^2 - kF_c^2|^2/\sum wF_o^4]^{1/2}$. [c] With hexadecapole terms of sulfur atoms.

of the neighboring molecule is shown in Figure 2a. There is a positive density accumulation in the N–H, N–C, C–S, and S–O bonds. The degree of density accumulation is in the order C–S > C–N, N–H > S–O. One of the O···H–N hydrogen bonds can be easily recognized in Figure 2a with the lone-pair density of the oxygen atom pointed toward the hydrogen atom. The plane perpendicular to Figure 2a, bisecting SO_2 and including the C–S bond, is depicted in Figure 3a. It is apparent that the lone-pair electron density of the sulfur atom is located at the apex of the trigonal pyramid extending toward the plane of SO_2 at the bisection of the O–S–O angle, which can also be detected in Figure 2a.

In addition to the normal refinement based on the spherical atom density model, a multipole atomic model refinement[11] in terms of a polynomial spherical harmonic series was also performed on this compound. The local Cartesian axes are indicated in Figure 1b. The improvements of the agreement indices over the various stages of expanding the series are illustrated in Table III. For the final results, terms up to the hexadecapole level are taken for all non-hydrogen atoms and only up to dipole terms for the hydrogen atoms. The final atomic parameters from this refinement are also given in Table II. The atomic scattering factors are calculated as the sum of core electron and valence electron scattering factors with coefficients taken from ref 13a. The He core is taken for C, N, and O, and the Ne core, for S. The valence configuration of C, N,O, and S are s^2p^2, s^2p^3,s^2p^4, and s^2p^4, respectively. The net atomic charges of the atoms obtained from the refinement with the multipole model are shown in Figure 1b with C, S, and H bearing positive charges and N and O negative charges. The model multipole deformation density distribution is obtained by Fourier synthesis with (F(multipole) – F(spherical)) as the coefficients. F(multipole) is calculated as described elsewhere.[11] F(spherical) is calculated from the same parameters as F(multipole) except that the coefficients of all the multipole terms are set to zero. The corresponding model deformation density maps are shown in Figures 2b and 3b. Figures 2c and 3c are so called pseudo static deformation density maps, where F(multipole) and F(spherical) are both calculated up to the same resolution of experimental maps with no thermal motion (thermal parameters set to zero). The features of the static and dynamic deformation density distributions are quite similar, but the static one has more pronounced peaks.

A simple EHMO calculation was also performed on this molecule with the aim of getting a theoretical deformation density map and atomic charge distribution. The net charges from such a calculation including d orbitals of the sulfur atom in the basis wave functions are shown in Figure 1b. The calculation without d orbitals in the basis set of the wave function not only yields much larger charges both on sulfur (+1.9) and oxygen (−1.42) atoms but also yields much less density along the S–C bond. Figures 2d and 3d are the calculated static deformation density maps according to the EHMO calculation.

Discussion

Because of the unusual length of the S–C bond in this structure, a polarized bond was proposed.[1,3] A recent report[17] indicates that the site of nucleophilic attack is either the sulfur atom or carbon atom of R_2CSO_2 depending on the substituent, R. This apparently supports the proposed polarization of the C–S bond, the direction of polarization C^-–S^+O_2 or C^+–S^-O_2 depending on the steric and electronic effects of the substituents on the carbon atom. The molecular dipole moment of thiourea in the 1:1 complex of thiourea with parabanic acid is in the direction of S→C.[18] Our

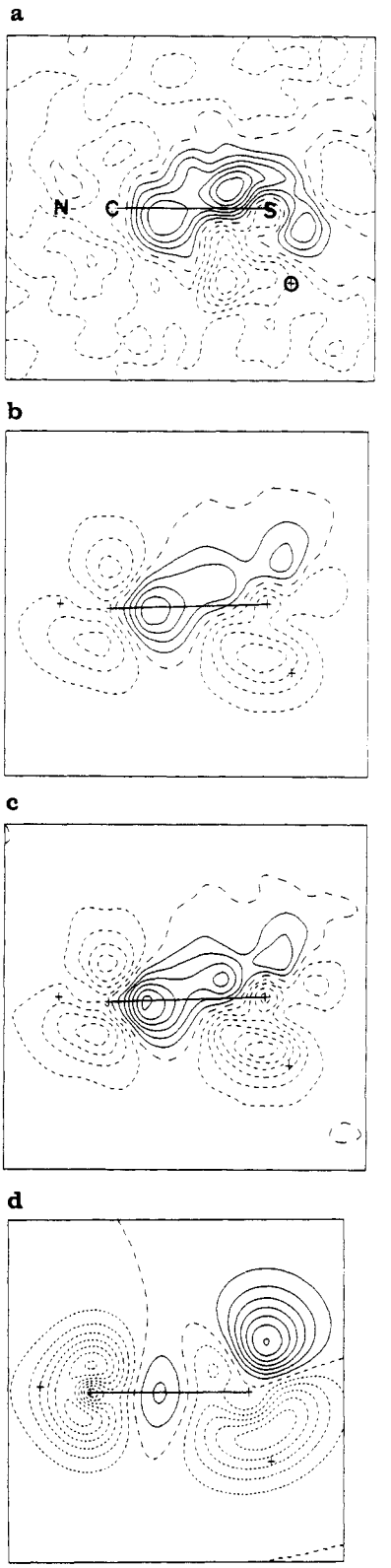

Figure 3. Deformation density maps of the plane perpendicular to that of Figure 2 but including the C–S bond (contour as in Figure 2; (a)–(d) defined as in Figure 2).

(17) Hartwig, U.; Pritzkow, H.; Rall, K.; Sundermeyer, W. *Angew Chem., Intl. Ed. Engl.* **1989**, *28*, 221.

(18) Weber, H. P.; Craven, B. M. *Acta Crystallogr., Sect. B: Struct. Sci.* **1987**, *B34*, 202.

results for the atomic charge distribution (Figure 1b) based on the multipole refinement are in good agreement with the following observations:[17,18] the H, C, and S atoms are positive, and the O and N atoms are negative. This is in accordance with what was proposed for $(H_2N)_2C^+$ with the positive charge mainly on H atoms and for SO_2^- with the electron density mainly polarized toward the oxygen atoms, leaving the S and C atoms slightly positive, which enables the nucleophilic attack.[17] The κ value of the H atom seems to be highly correlated with its net charge. The result here is from the fixed κ value of 1.4. This gives the least correlation between dipole terms of H and those of the N atom. The bond lengths (Figure 1a) at low temperature are longer than those of at room temperature, as expected for the thermal motion differences.[19,20] However, the C-S length, on the contrary, is shortened somewhat. A similar phenomenon has been observed in other related sulfur bond lengths.[16] The S-O distance is longer than a localized double bond,[15] and the C-N distance is comparable to a partially double bond. The C-S bond is slightly longer than the single bond. Thus, the geometry of the structure itself reveals the charge polarization of the form proposed previously.[1,3]

The experimental deformation density distribution of thiourea *S,S*-dioxide in the plane of thiourea appears to be quite similar to that of thiourea,[6] and the density accumulation along the C-S bond is slightly polarized toward the C atom indicating S→C. Although both atoms are positive, the carbon atom is less positive than the sulfur atom. The density accumulation along the N-H and C-N bonds is as expected. The loss of density near the sulfur nucleus has been found in other sulfur-containing compounds.[15,16,21] This also agrees well with the atomic net charges obtained from the multipole refinement. The density accumulation along the S-O bonds is less apparent or more diffuse than that of other experimental results.[15] This may be due to the fact that each oxygen atom accepts two intermolecular hydrogen bonds in the crystal. It is interesting to notice that, in the dynamic multipole deformation density map of Figure 2b, the density along the S-O bond is less diffuse and polarized more toward the oxygen atoms (thus yielding a relatively large negative charge for the oxygen atom) than that of the experimental one (Figure 2a). Nevertheless, the H-bonds are still clearly observed in the multipole deformation density map, in spite that the multipole model is a better representation near the nucleus and in the intramolecular bonded atom region. The influence of the intermolecular H-bonding on the electron distribution has been noticed and studied recently.[22] Similarly, the lone-pair density at the sulfur atom is better represented in the multipole deformation density map (Figure 3b) than in the experimental one (Figure 3a) and is comparable to that of the theoretically calculated one (Figure 3d). The pseudo static deformation density distribution (Figures 2c and 3c) gives the deformation density distribution without the thermal smearing effect at the same resolution level. The resemblance between the dynamic and static deformation density distributions indicates little correlation between thermal motion and the deformation density.

In order to see the effect of each multipole term on the deformation density distribution, a multipole density map was produced at each step of expanding the multipole terms on all the atoms. It was obvious that, at least, all terms up to the quadrupole terms are needed for building up the density between the bonded atoms. Adding octapole terms certainly improved the density accumulation significantly. Additional hexadecapole terms on the C, N, and O atoms improved the density accumulation only slightly; however, this term was important for the sulfur atom.

The net atomic charges from the EHMO calculation given in Figure 1b are in agreement with the ones obtained by the multipole refinement. The deformation density based on the EHMO calculation only provides a qualitative comparison. The small basis set calculations such as those with EHMO often underestimate the deformation density in the bonding regions but overestimate it in the lone-pair regions. A more sophisticated ab initio calculation of the title compound is underway.

Conclusion

Deformation density studies of thiourea dioxide, both by direct inspection of an experimental deformation density map and by construction of it according to a multipole model, lead to a better understanding of the atomic net charge distribution of the molecule. The need of up to octapole terms for building up the density in the bonds is confirmed. The extra hexadecapole term is important for the sulfur atom, which implies the angular complexity of the electronic distribution of sulfur atom in the molecule. The intermolecular H-bonding effect is observable in both the experimental and model deformation density maps. Simple EHMO calculations can provide a qualitative comparison.

Acknowledgment. We wish to thank the National Science Council of the Republic of China for financial support. Thanks are also due to Professor Coppens for supplying the MOLLY program. We also express our appreciation to Dr. C. H. Ueng and Mr. G. H. Lee for their help on the low-temperature data collection and to Mr. H. C. Lin for software support.

Registry No. $(H_2N)_2CSO_2$, 4189-44-0.

Supplementary Material Available: Tables SI-SIII, listing complete crystal data, atomic thermal parameters from various refinements, and coefficients of atomic multipole terms up to the hexadecapole level for non-hydrogen atoms and to the dipole level for hydrogen atoms (3 pages); Table SIV, listing calculated and observed structure factors (11 pages). Ordering information is given on any current masthead page.

(19) Busing, W. R.; Levy, H. A. *Acta Crystallogr.* **1964**, *17*, 142.
(20) Wang, Y.; Blessing, R. H.; Ross, F.; Coppens, P. *Acta Crystallogr., Sect. B: Struct. Crystallogr. Cryst. Chem.* **1976**, *B32*, 572.
(21) Wang, Y.; Liao, J. H. *Acta Crystallogr., Sect. B: Struct. Sci.* **1989**, *B45*, 65.
(22) Kring, M. P. C. M.; Graafsma, H.; Feil, D. *Acta Crystallogr., Sect. B: Struct. Sci.* **1988**, *B44*, 609.

Contribution from the Fachbereich Chemie, Universität Dortmund, 4600 Dortmund, Federal Republic of Germany

Head-Tail Oriented Nucleobases (B = Guanine, Cytosine) in *cis*-A_2PtB_2 Resisting Cyanide Substitution. Implications for the Nature of Strongly DNA-Bound Cisplatin

Gudrun Frommer and Bernhard Lippert*

Received June 7, 1989

The adducts formed by the antitumor agent *cis*-diamminedichloroplatinum(II), *cis*-DDP (Cisplatin), with DNA cannot be completely removed even with excess cyanide.[1] Model nucleobase complexes of *cis*-DDP exhibit quite substantial differences in substitution rates when treated with CN^-. These observations have led us to speculate that cross-links other than those between two guanines on one DNA strand (intrastrand G,G adduct) might account for this phenomenon.[2] Specifically, the protective effect of the exocyclic oxygens of N3-bound thymine (and likewise uracil) ligands has been noted. It was suggested that the electron lone pairs of the carbonyl oxygens at either side of the Pt coordination plane in uracil and thymine complexes were responsible for this phenomenon. These oxygens are positioned such as to make an associative substitution mechanism difficult. In contrast, the two 9-ethylguanine (9-EtGH) ligands in *cis*-$[(NH_3)_2Pt(9\text{-EtGH-}N^7)_2]^{2+}$, which, in the solid state, are arranged head-head[3] very

(1) (a) Stone, P. J.; Kelman, A. D.; Sinex, F. M. *Nature* **1974**, *251*, 736. (b) Munchhausen, L. L.; Rahn, R. O. *Biochim. Biophys. Acta* **1975**, *414*, 242. (c) Lippard, S. J.; Hoeschele, J. D. *Proc. Natl. Acad. Sci. U.S.A.* **1979**, *76*, 6091. (d) Tullius, T. D.; Lippard, S. J. *J. Am. Chem. Soc.* **1981**, *103*, 4620. (e) Ushay, H. M.; Tullius, T. D.; Lippard, S. J. *Biochemistry* **1981**, *20*, 3744. (f) Bauer, W.; Gonias, S. L.; Kam, S. K.; Wu, K. C.; Lippard, S. J. *Biochemistry* **1978**, *17*, 1060. (g) Leng, M. Personal communication.
(2) Raudaschl-Sieber, G.; Lippert, B. *Inorg. Chem.* **1985**, *24*, 2426.
(3) (a) Lippert, B.; Raudaschl, G.; Lock, C. J. L.; Pilon, P. *Inorg. Chim. Acta* **1984**, *93*, 43. (b) Schöllhorn, H.; Raudaschl-Sieber, G.; Müller, G.; Thewalt, U.; Lippert, B. *J. Am. Chem. Soc.* **1985**, *107*, 5932.

0020-1669/90/1329-3259$02.50/0